Applied Physics A (2020) 126:26
https://doi.org/10.1007/s00339-019-3208-2

Applied Physics A
Materials Science & Processing

Influence of PVP polymer concentration on nonlinear absorption in silver nanoparticles at resonant excitation

Sandeep Kumar Maurya[1] · Rashid A. Ganeev[1] · Anuradha Rout[1] · Chunlei Guo[1,2]

Received: 25 August 2019 / Accepted: 3 December 2019 / Published online: 12 December 2019

Abstract
Silver nanoparticles exhibit saturable absorption at resonant excitation, which upon addition of the polymer as a capping agent, exhibit reverse saturable absorption. These nonlinear optical processes play an important role in the overall nonlinear optical properties of silver nanoparticle. Thus, with this viewpoint, the nonlinear absorption of silver nanoparticles in deionized water in the presence of varying concentration polyvinylpyrrolidone polymer was investigated using femtosecond laser pulses at 400 nm. This study shows that the saturable absorption process is significantly suppressed at high concentration of the polymer. The silver nanoparticle with smaller size shows pure reverse saturable absorption process with the respective coefficient of $\beta = 7.55 \times 10^{-12}$ cm/W. The change in the nonlinear optical response from combined saturable absorption and reverse saturable absorption to pure reverse saturable absorption process was observed as the concentration of polymer increases.

1 Introduction

The optical nonlinearities in nanoparticles (NPs) are of utmost importance due to its potential applications in nanotechnology, optical signal processing and optical communication devices [1–6]. NPs exhibit strong surface plasmon resonance (SPR) due to the reduced dimensionality as compared to the bulk materials. This leads to the giant nonlinear optical response upon interaction with high-power laser pulses at a frequency close to the SPR due to enhancement in the local electric field near the surface of NPs. At resonant excitation of optically active materials, the various nonlinear optical processes such as saturable absorption (SA), reverse saturable absorption (RSA), occurs depending on the employed laser pulse energy [7, 8]. SA is the process which occurs in the medium at sufficiently high intensity of laser pulses, which leads to the depletion of ground state. This occurs in the optically active medium, where excited state absorption cross-section is lower than the ground state absorption cross-section at the employed wavelength. However, RSA occurs when excited state absorption probability is higher as compared to ground state absorption at the high intensity of laser pulses, which lead to the multiphoton excitation depending on the wavelength. The variations in the shape, size, and optical properties of NPs lead to the enhanced functionality towards their photonics and biomedical device applications [9, 10].

Silver (Ag) metal NPs have been thoroughly studied for the enhanced third-order nonlinear optical properties due to their SPR characteristics at resonant excitation. The nonlinear optical characteristics of Ag NPs suspensions in different solvent exhibit optical switching of the SA to RSA at high power of incident laser pulses [11]. The optical nonlinearity in NPs depends on the size, which can alter the contribution of SA and RSA process to overall nonlinear optical response at the resonant condition. A variety of methods have been implemented for the synthesis of Ag NPs [12–21]. Among them, the chemical reduction approach of Ag^+ ion is most popular due to its simplicity, low cost and ability to produce large quantities. In the chemical reduction method, the size of the NPs can be adjusted by controlling the reaction condition such as temperature, reducing agent and capping agents etc. [22]. There are several reports on the effect of reducing agents and stabilizing agents on the morphology of Ag NPs using the chemical reduction [23–29]. But there are rarely

✉ Chunlei Guo
guo@ciomp.ac.cn; guo@optics.rochester.edu

[1] The Guo China-US Photonics Laboratory, State Key Laboratory of Applied Optics, Changchun Institute of Optics, Fine Mechanics and Physics, Chinese Academy of Sciences, Changchun 130033, China

[2] The Institute of Optics, University of Rochester, Rochester, NY 14627, USA

few reports based on the varying concentration of the protective agent to regulate the size of the NPs [30, 31]. Most of the studies related to the effect of the protecting agent were performed for metal NPs doped in polymer metrix [32–35]. There is a lack of information about the switching mechanism from SA to RSA process in the presence of polymer. The nonlinear optical response in NPs shows the combined influence of SA and RSA processes depending on the employed laser parameter. Ag NPs were found to exhibit SA upon 400 nm excitation, whereas in polymer matrix such as polyvinylpyrrolidone (PVP) [35], exhibit pure RSA process at 400 nm. This can provide the possibility to investigate the role of PVP polymer on the nonlinear optical response of Ag NPs suspension.

Thus, with this viewpoint, the nonlinear optical properties of synthesized Ag NPs in deionized water with varying concentration of PVP polymer by a chemical reduction method have been studied using femtosecond laser pulses at 400 nm. The effect of polymer concentration on the nonlinear optical characteristics for synthesized Ag NPs is investigated and discussed in detail.

2 Experimental details

Materials used in the preparation of Ag NPs suspensions were spectroscopic grade 99.99% pure PVP polymer with molecular weight $M_w = 40{,}000$ and polymerization number $n = 360$ (PVP K30), silver nitrate ($AgNO_3$) and sodium borohydride (SBH). Ag NPs suspension in deionized water was prepared by chemical reduction of $AgNO_3$ from SBH in the presence of PVP polymer. To prepare Ag NPs in deionized water, at first, 0.043 g of $AgNO_3$ was dissolved in 50 mL deionized water and 0.012 g of SBH was dissolved in 150 mL deionized water with constant stirring for 30 min. The 0.1 mL of aqueous $AgNO_3$ solution was gently mixed into 10 mL of aqueous SBH solution in the presence of PVP polymer using constant stirring at room temperature. The mixture was stirred for 30 min, which allow $AgNO_3$ and SBH to react completely in the presence of PVP polymer. Ag NPs with varying concentration of PVP were prepared for the measurement of nonlinear optical response, where final concentration of polymer in Ag NPs suspensions was achieved to be 0 mg/L (S1), 0.1 mg/L (S2), 0.5 mg/L (S3), 1 mg/L (S4), 2 mg/L (S5) and 3 mg/L (S6). The prepared Ag NPs with varying strength of PVP were characterized using UV–Visible spectrometer (Cary Series, Agilent technologies) and scanning electron microscope (SEM, Hitachi S-4800).

Nonlinear optical properties of the prepared Ag NPs in deionized water were measured using conventional open aperture Z-scan technique [36] at 400 nm. The laser pulse at 400 nm was obtained by upconversion of 800 nm laser pulse from the regenerative amplifier (Spitfire ACE, spectra physics, 800 nm, 1 kHz), which was seeded by Ti: Sapphire laser running at 800 nm, 43 MHz. The pulse width of the femtosecond laser pulse was fixed at 35 fs measured using a noncollinear autocorrelation technique which was further confirmed by measurement using commercially available autocorrelator. The quartz cuvette of 1 mm path length was used for the measurement of nonlinear optical properties of Ag NPs suspension. The cuvette containing Ag NPs suspension was moved across the focal plane of the plano-convex lens of focal length 400 mm along the beam propagation direction by mean of the motorized translational stage. The propagated pulses through sample cuvette containing Ag NPs suspension were detected using large-area photodiode (DET100A/M, Thorlabs). Beam diameter of femtosecond laser pulses at the focus was 72 μm which was measured using beam profilometer.

3 Results and discussion

Figure 1a shows the optical absorption spectra of Ag NPs and PVP dispersed in deionized water, where S1 shows SPR band at 404 nm with sideband at 350 nm. On the other hand, PVP does not show any absorption in the region 250–800 nm. Figure 1b shows the absorption spectra of prepared Ag NPs with varying concentration of PVP polymer. As the concentration of PVP increases, SPR associated with Ag NPs appears at 396 nm which is a blue shift by ~ 8 nm as compared to Ag NPs in deionized water in the absence of PVP.

In addition to SPR bands in Ag NPs, the sidebands in the region of 500–900 nm also appear. These absorption bands arise due to the presence of irregular shape and size of the Ag NPs in deionized water. Under the assumption of Mie theory, spherical NPs possess single band representing SPR [37]. Whereas the secondary absorption band between 500 and 800 nm appears due to the presence of non-spherical NPs [38], which corresponds to the dipole and quadrupole modes of Ag. This is due to the fact that the discretization of conduction and valance bands with degeneracy occurs which depends on their shape and size [39, 40]. It is experimentally and theoretically shown in the literature [41] that the absorption band in the region of 500–900 nm appears as the shape of the Ag NPs changes. Another possible reason for the appearance of a broad absorption band across the entire visible spectrum could be the aggregation of smaller size Ag NPs [42]. It was observed that as the concentration of PVP increases, absorption band in near-IR region for Ag NPs suspension in deionized water is shifted to the blue region toward the principle SPR band at 396 nm. This is due to the influence of the size of the prepared Ag NPs in the presence of PVP as shown in respective SEM images (see

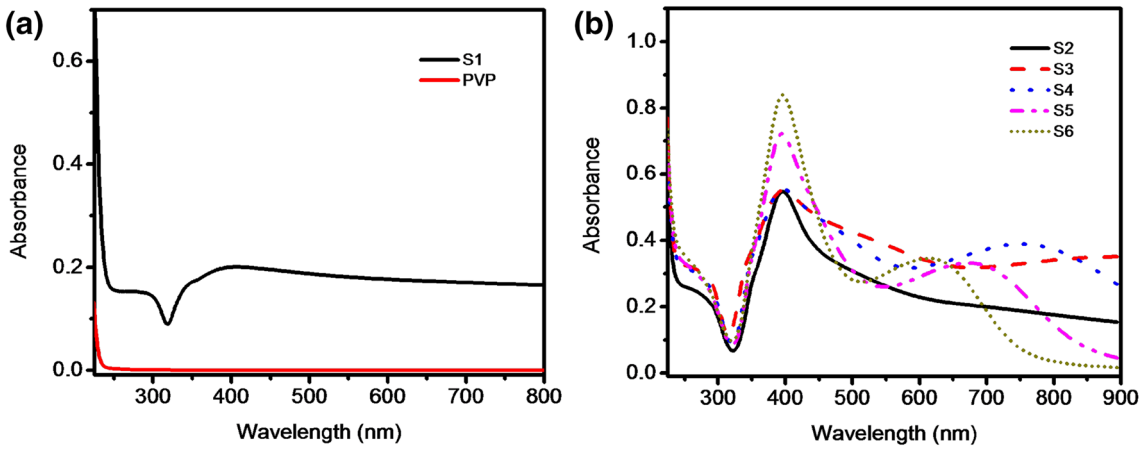

Fig. 1 Absorption spectra of Ag NPs in deionized water with varying concentration of PVP polymer, where S1, S2, S3, S4, S5 and S6 represent the concentration of PVP polymer of 0 mg/L, 0.1 mg/L, 0.5 mg/L, 1 mg/L, 2 mg/L and 3 mg/L, respectively

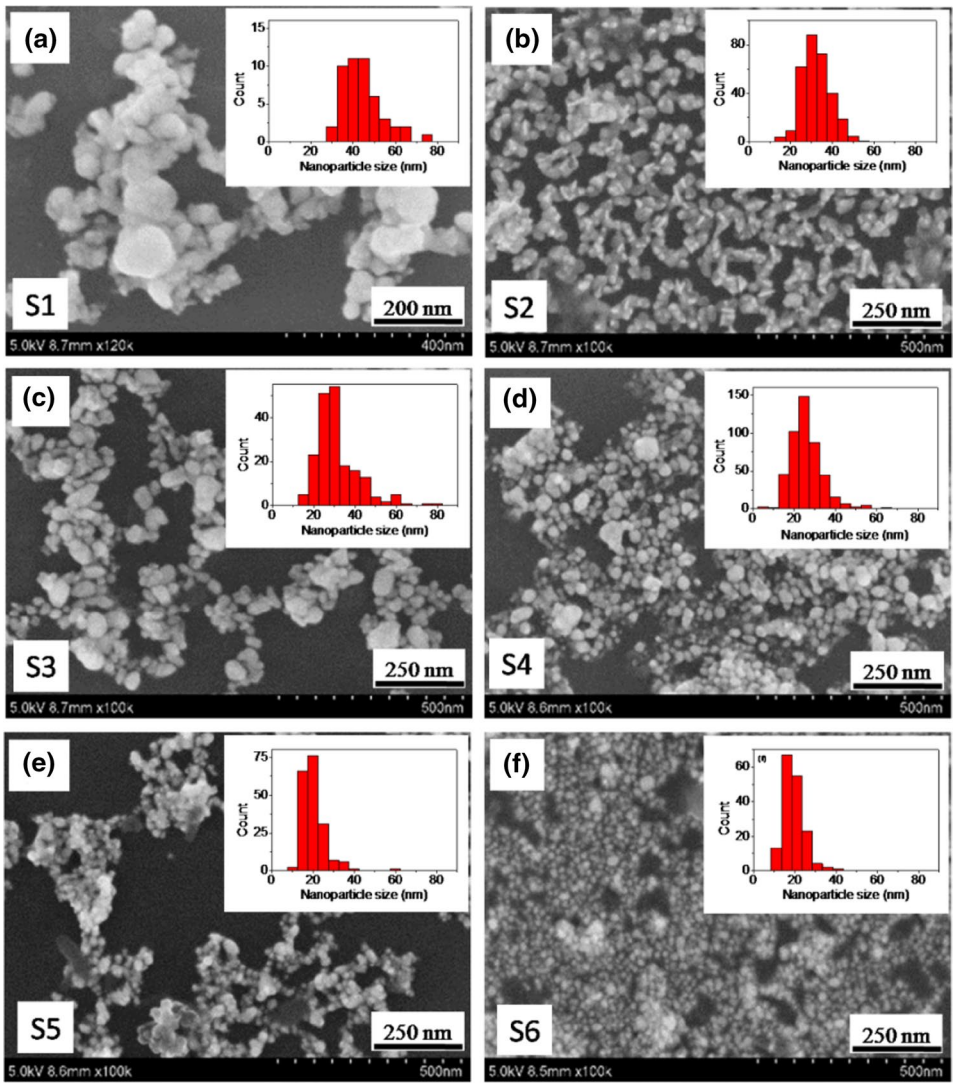

Fig. 2 SEM images of chemically prepared Ag NPs in deionized water with a varying concentration of PVP with their respective particle size distribution in insets. **a** S1, **b** S2, **c** S3, **d** S4, **e** S5 and **f** S6

Fig. 2). It was observed that as the concentration of PVP increases, the size of the Ag NPs decreases. Hence, the blue shift is imminent.

The nonlinear optical properties in Ag NPs in suspensions were measured using an open aperture Z-scan experiment at the intensity of 9.3×10^{10} W/cm^2. Figure 3a shows the transmittance profile of the open aperture Z scan trace for S1 which reflects the combined influence of SA and RSA in the transmittance profile at 400 nm in Ag NPs in the absence of PVP polymer. The increase in transmittance was observed as the sample moves towards the focus as shown in Fig. 3a. It was observed that transmittance started to decrease after certain z position and change in transmittance shows the valley around $Z=0$. A similar trend was observed for the sample S2, S3, and S4, where polymer concentration was increased gradually up to 1 mg/L (see Fig. 3b–d). The sample S5 and S6 show only the RSA process as the concentration of PVP increases beyond 1 mg/L as shown in Fig. 3e, f. At the maximum employed pulse intensity of 9.3×10^{10} W/cm^2, nonlinear optical response from empty quartz cuvette and cuvette containing 3 mg/L of PVP in deionize water were not observed at 400 nm. These results indicate that the nonlinear optical effects in suspension are only due to Ag NPs and PVP polymer influencing the size of Ag NPs.

$$T_{\mathrm{SA,RSA}}=\left(1-\frac{\beta I_0 L_{\mathrm{eff}}}{2\sqrt{2}\left(1+x^2\right)}\right)\times\left(1+\frac{I_0}{I_{\mathrm{sat}}(1+x^2)}\right) \quad (1)$$

The nonlinear absorption parameters, I_{sat} and β, for Ag NPs suspensions in deionized water were determined using Eq. 1 [43], where $x=z/z_0$, I_0 is the peak intensity of the laser pulse, I_{sat} is the saturation intensity of the optically active medium which depends on the concentration of the medium, β is the RSA coefficient, z_0 is the Rayleigh length defined as $z_0=k(w_0^2)/2$, w_0 is the radius of the focused beam, $L_{\mathrm{eff}}=[1-\exp(-\alpha_0 L)]/\alpha_0$ is the effective length of the medium, α_0 is the linear absorption coefficient of the medium. Equation 1 represents the combined influence of

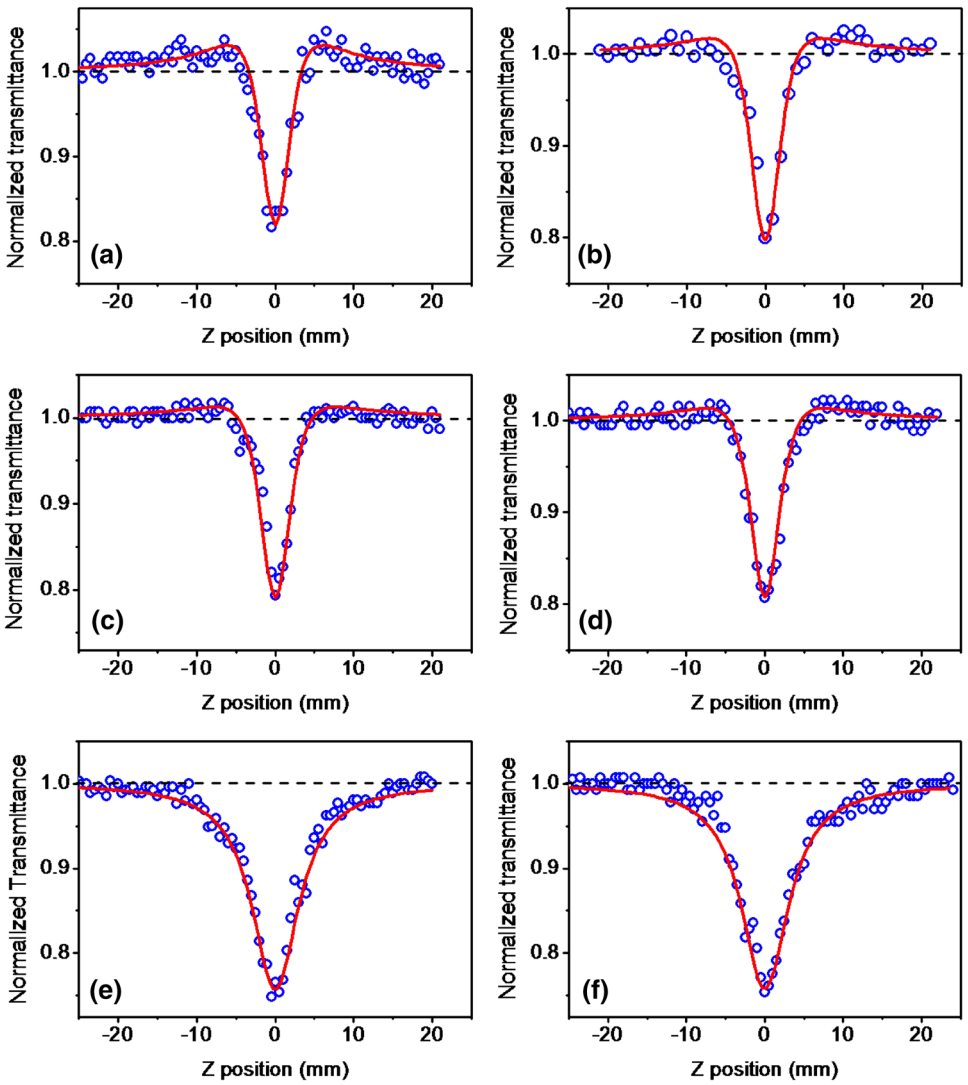

Fig. 3 Open aperture z scan traces for chemically prepared Ag NPs with varying concentration of PVP polymer at the peak intensity of 9.3×10^{10} W/cm^2 at 35 fs, 400 nm. **a** S1, **b** S2, **c** S3, **d** S4, **e** S5 and **f** S6. The open circle and solid line represent the experimental data and theoretical fit, respectively. Error bar in trace of open aperture Z-scan in **b** to **f** is similar to **a**. The dashed line represents the normalized transmittance $T=1$

RSA and SA associated with Ag NPs. The first fraction in the equation represents the RSA process which is responsible for the valley in the transmittance profile around focus, whereas the second fraction represents the formalism of the SA process, which is responsible for the increase in transmittance over unity. The determined value of I_{sat} and β for S1 representing Ag NPs in deionized water was 1×10^{12} W/cm^2 and 8.2×10^{-12} cm/W, respectively. Whereas the β value for sample S6 was $\beta = 7.55\times10^{-12}$ cm/W which represents RSA in Ag NPs with the polymer concentration of 2 mg/L. The second fraction in Eq. 1 was fixed to 1 while fitting of Z scan trace for sample S5 and S6, since SA process was not observed. The obtained nonlinear optical parameters were found to be consistent with our previously reported Ag NPs at 400 nm [44]. There are several reports on the transition from SA to RSA in Ag NPs with the decrease in the size on or near-resonance condition [45].

For the case of Ag NPs, the presence of SA arises due to saturation of excited state population through intraband (occupied sp → unoccupied sp) transition at resonant excitation with reasonable high intensity shown in arrow 1 of Fig. 4, which results in the photo-bleaching of the ground state at the employed laser pulse energy. At the same time, one photon transition probability for PVP polymer is also possible through $\pi \rightarrow n\pi^*$ transition at 400 nm [42] which can contribute to the overall SA process shown in arrow 3 of Fig. 4. To validate that there is no influence of PVP at the optical nonlinearity of Ag NP in suspension at 400 nm, the nonlinear optical response from 3 mg/L PVP polymer suspended in deionized water was measured using open aperture Z scan at the maximum employed fluence, which shows absence of optical nonlinearity in PVP suspension. The threshold of SA process in nanoparticle suspension can increase as the polymer concentration increases, which possibly occur due to the presence of additional transition probability in the polymer alongside one-photon transition in Ag NPs at 400 nm. On the other hand, RSA in Ag NPs can occur through simultaneous absorption of two-photons through interband (occupied d → unoccupied sp, see arrow 2 of Fig. 4). However, upon excitation with 400 nm, excited Ag NPs can transfer its energy to PVP through non-radiative pathways, which can probably reduce the efficiency of SA in Ag NPs.

Figure 5a shows the SA intensity and RSA coefficient as a function of PVP concentration. The pure RSA was observed beyond the PVP concentration of 1 mg/L. The variation in RSA coefficients is possibly the effect of size of the Ag NPs. Figure 5b shows the variation of RSA coefficient as a function of mean size of the Ag NPs in suspension, which was determined using respective SEM images of prepared Ag NPs. It is evident that RSA coefficient increases as the size of the NPs increases, which was found to be in good agreement with literature [46]. The

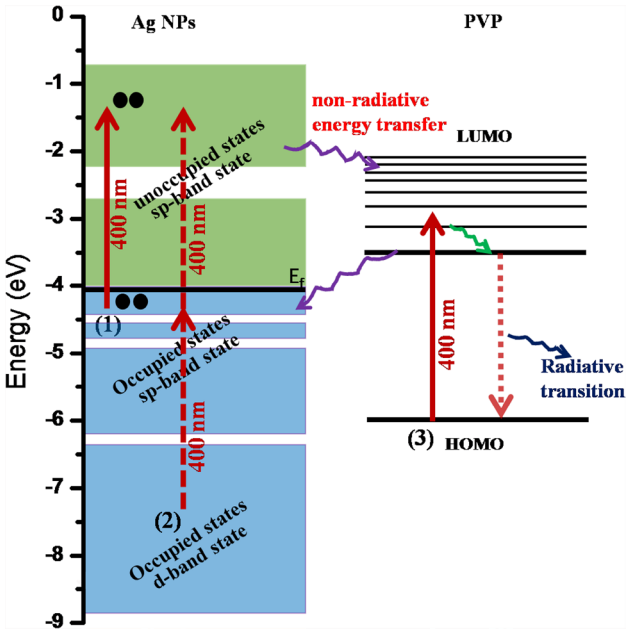

Fig. 4 Schematic of electronic excitation for Ag NPs and PVP in the water with excitation at 400 nm [44, 47]. The black circular dots represent the equal population in the lower and upper electronic state reflecting the absorption saturation in Ag NPs. The solid upward arrow represents excitation using 400 nm (3.1 eV) and the dotted downward arrow represents possible radiative transition at a longer wavelength. Whereas the two-photon transition is represented by upward dashed arrow. E_f represents the energy associated with the Fermi level in eV for Ag NPs. The blue-colored arrow represents the non-radiative energy transfer during the relaxation process, which is known as intersystem crossing whereas green colored arrow represents the internal conversion in PVP

nonlinear absorption in NPs consists of various processes such as transient absorption, photo ejection by multi-photon absorption, interband and intraband transitions and nonlinear scattering. At the high intensity of laser pulses, the transient absorption from free carriers becomes substantial which can be accompanied by the photo ejection of an electron through the multi-photon absorption process. Thus, RSA is imminent which can prevail the SA process. Upon increase of the laser intensity by moving the sample toward the focus of the focusing lens, TPA processes are also imminent due to the possibility of multi-photon intraband and interband transition in Ag NPs. In the case of Ag, the energy required for d → sp interband transitions has to be higher than 4 eV for Ag NPs. Under our experimental condition, the wavelength of the employed photon is 400 nm which is equivalent to the 3.2 eV. The multiphoton absorption is possible under the high-intensity regime at 400 nm excitation. Thus, the observed RSA can be directly attributed to the interband d → sp transition which occurs in addition to SA process.

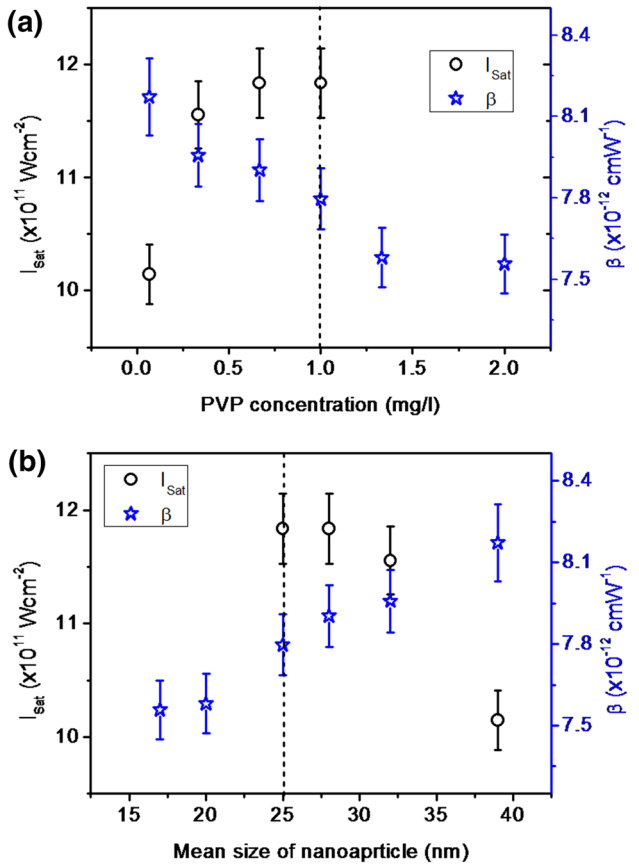

Fig. 5 Variation of I_{sat} and β with varying **a** concentration of PVP polymer and **b** mean size of the nanoparticle at 400 nm, 35 fs

4 Conclusions

We have reported the effect of PVP polymer on the nonlinear optical absorption of Ag NPs in deionized water using femtosecond laser pulses at 400 nm. It was observed that the polymer concentration plays a significant role in nonlinear optical properties of Ag NPs. This study shows that saturable absorption has a dominating factor for higher concentration of Ag NPs over the RSA process at resonance excitation. It is evident from the nonlinear optical characterization of Ag NPs that NPs possessing high intensity of saturation absorption has low RSA coefficient which depends on their size. The I_{sat} and β for Ag NPs in absence of PVP polymer deionized water were 1×10^{12} W/cm^2 and 8.2×10^{-12} cm/W, respectively. Whereas pure RSA with $\beta = 7.55 \times 10^{-12}$ cm/W was observed as the concentration of PVP was increased beyond 1 mg/L. The addition of PVP polymer acts as inhibitors for the SA process because of the presence of lower-lying energy states for PVP which can also undergo one-photon transition at off-resonant excitation at 400 nm. This study suggest that the material having RSA can also be used as an optical limiter to protect optical sensors from high-power laser pulses.

Acknowledgements The research was supported by the National Key Research and Development Program of China (2018YFB1107202, 2017YFB1104700), The financial support from the Natural Science Foundation of China (91750205, 11774340, 11804334), K. C. Wong Education Foundation (GJTD-2018-08) and Jilin Provincial Science & Technology Development Project (20180414019GH).

References

1. Y.-X. Zhang, Y.-H. Wang, Nonlinear optical properties of metal nanoparticles: a review. RSC Adv. **7**, 45129 (2017)
2. V.V. Mody, R. Siwale, A. Singh, H.R. Mody, Introduction to metallic nanoparticles. J. Pharm. Bioallied Sci. **2**, 282 (2010)
3. N.I. Zheludevn, Nonlinear optics on the nanoscale. Contemp. Phys. **43**, 365 (2002)
4. K. Xu, C. Zhang, R. Zhou, R. Ji, M. Hong, Hybrid micro/nanostructure formation by angular laser texturing of Si surface for surface enhanced Raman scattering. Opt. Exp. **24**, 10352 (2016)
5. K. Xu, H. Yan, C.F. Tan, Y. Lu, Y. Li, G.W. Ho, R. Ji, M. Hong, Hedgehog inspired CuO nanowires/Cu_2O composites for broadband visible-light-driven recyclable surface enhanced Raman scattering. Adv. Opt. Mater. **6**, 1701167 (2018)
6. K. Xu, R. Zhou, K. Takei, M. Hon, Toward flexible surface-enhanced Raman scattering (SERS) sensors for point-of-care diagnostics. Adv. Sci. **6**, 1900925 (2019)
7. Y. Gao, W. Wu, D. Kong, L. Ran, Q. Chang, H. Ye, Femtosecond nonlinear absorption of Ag nanoparticles at surface plasmon resonance. Physica **45**, 162 (2012)
8. H.H. Mai, V.E. Kaydashev, V.K. Tikhomirov, E. Janssens, M.V. Shestakov, M. Meledina, S. Turner, G.V. Tendeloo, V.V. Moshchalkov, P. Lieven, Nonlinear optical properties of Ag nanoclusters and nanoparticles dispersed in a glass host. J. Phys. Chem C **118**, 15995 (2014)
9. P.C. Ray, Size and shape dependent second order nonlinear optical properties of nanomaterials and their application in biological and chemical sensing. Chem. Rev. **110**, 5332 (2010)
10. K.L. Kelly, E. Coronado, L.L. Zhao, G.C. Schatz, The optical properties of metal nanoparticles: the influence of size, shape, and dielectric environment. J. Phys. Chem. B **107**, 668 (2003)
11. M. Hari, S. Mathew, B. Nithyaja, S.A. Joseph, V.P.N. Nampoori, P. Radhakrishnan, Saturable and reverse saturable absorption in aqueous silver nanoparticles at off-resonant wavelength. Opt. Quantum Electron. **43**, 49 (2012)
12. X.-F. Zhang, Z.-G. Liu, W. Shen, S. Gurunathan, Silver nanoparticles: synthesis, characterization, properties, applications, and therapeutic approaches. Int. J. Mol. Sci. **17**, 1534 (2016)
13. T. Tsuji, K. Iryo, Y. Nishimura, M. Tsuji, Preparation of metal colloids by a laser ablation technique in solution: influence of laser wavelength on the ablation efficiency (II). J. Photochem. Photobiol. A Chem. **145**, 201 (2001)
14. T. Tsuji, K. Iryo, N. Watanabe, M. Tsuji, Preparation of silver nanoparticles by laser ablation in solution: influence of laser wavelength on particle size. Appl. Surf. Sci. **202**, 80 (2002)
15. Z. Shervani, Y. Ikushima, M. Sato, H. Kawanami, Y. Hakuta, T. Yokoyama, T. Nagase, H. Kuneida, K. Aramaki, Morphology and size-controlled synthesis of silver nanoparticles in aqueous surfactant polymer solutions. Colloid Polym. Sci. **286**, 403 (2007)
16. D.C. Tien, C.Y. Liao, J.C. Huang, K.H. Tseng, J.K. Lung, T.T. Tsung, W.S. Kao, T.-H. Tsai, T.-W. Cheng, B.-S. Yu, H.-M. Lin, L. Stobinski, Novel technique for preparing a nano-silver water

suspension by the arc-discharge method. Rev. Adv. Mater. Sci. **18**, 752 (2008)
17. J.Y. Song, B.S. Kim, Rapid biological synthesis of silver nanoparticles using plant leaf extracts. Bioprocess. Biosyst. Eng. **32**, 79 (2008)
18. J. Natsuki, T. Natsuki, Y. Hashimoto, A Review of silver nanoparticles: synthesis methods, properties, and applications. I. J. Mat. Sci. Appl. **4**, 325 (2015)
19. S. Agnihotri, S. Mukherji, S. Mukherji, Size-controlled silver nanoparticles synthesized over the range 5–100 Nm using the same protocol and their antibacterial efficacy. RSC Adv. **4**, 3974 (2014)
20. H.R. Ghorbani, A.A. Safekordi, H. Attar, S.M. Sorkhabadi, Biological and non-biological methods for silver nanoparticles synthesis. Chem. Biochem. Eng. Q. J. **25**, 317 (2011)
21. H. Wang, X. Qiao, J. Chena, S. Ding, Preparation of silver nanoparticles by chemical reduction method. Colloids Surf. A Physicochem. Eng. Asp. **256**, 111 (2005)
22. Y.C. Lu, K.S. Chou, A simple and effective route for the synthesis of nano-silver colloidal dispersions. J. Chin. Inst. Chem. Eng. **39**, 673 (2008)
23. G. Guo, W. Gan, J. Luo, F. Xiang, J. Zhang, H. Zhou, H. Liu, Preparation and dispersive mechanism of highly dispersive ultrafine silver powder. Appl. Surf. Sci. **256**, 6683 (2010)
24. D. Wang, C. Song, Z. Hu, X. Zhou, Synthesis of silver nanoparticles with flake-like shapes. Mater. Lett. **59**, 1760 (2005)
25. Z. Zhang, B. Zhao, L. Hu, PVP protective mechanism of ultrafine silver powder synthesized by chemical reduction processes. J. Solid State Chem. **121**, 105 (1996)
26. B. He, J.J. Tan, K.Y. Liew, H. Liu, Synthesis of size controlled Ag nanoparticles. J. Mol. Catal. A Chem. **221**, 121 (2004)
27. H. Wang, X. Qiao, J. Chen, X. Wang, S. Ding, Mechanisms of PVP in the preparation of silver nanoparticles. Mater. Chem. Phys. **94**, 449 (2005)
28. J. Natsuki, T. Natsuki, Y. Hashimoto, A review of silver nanoparticles: synthesis methods, properties and applications. Int. J. Mater. Sci. Appl. **4**, 325 (2015)
29. H.D. Beyene, A.A. Werkneh, H.K. Bezabh, T.G. Ambaye, Synthesis paradigm and applications of silver nanoparticles (AgNPs) a review. Sustain. Mater. Technol. **13**, 18 (2017)
30. L. Gharibshahi, E. Saion, E. Gharibshahi, A.H. Shaari, K.A. Matori, Influence of Poly(vinylpyrrolidone) concentration on properties of silver nanoparticles manufactured by modified thermal treatment method. PLoS ONE **12**, e0186094 (2017)
31. T.M.D. Dang, T.T.T. Le, E. Fribourg-Blanc, M.C. Dang, Influence of surfactant on the preparation of silver nanoparticles by polyol method. Adv. Nat. Sci.: Nanosci. Nanotechnol. **3**, 035004 (2012)
32. M. Ghanipour, D. Dorranian, Effect of Ag- Nanoparticle doped in polyvinyl alcohol on the structural and optical properties of PVA film. J. Nanomater. **2013**, 897043 (2013)
33. N. Misra, M. Rapolu, S.V. Rao, L. Varshney, V. Kumar, Nonlinear optical studies of inorganic nanoparticles polymernanocomposite coatings fabricated by electron beam curing. Opt. Laser Tech. **79**, 24 (2016)
34. L.-D. Wang, T. Zhang, X.-Y. Zhang, Y.-J. Song, R.-Z. Li, S.-Q. Zhu, Optical properties of Ag nanoparticle-polymer composite film based on two-dimensional Au nanoparticle array film. Nanoscale Res. Lett. **9**, 155 (2014)
35. A.L. Stepanov, Nonlinear optical properties of implanted metal nanoparticles in various transparent matrixes: a review. Rev. Adv. Mater. Sci. **27**, 115 (2011)
36. M. Sheik-bahae, A.A. Said, T.-H. Wei, D.J. Hagan, E.W.V. Stryland, Sensitive measurement of optical nonlinearities using a single beam. IEEE J. Quantum Electron. **26**, 760 (1990)
37. G. Mie, Articles on the optical characteristics of turbid tubes, especially colloidal metal solutions. Ann. Phys. **25**, 377 (1908)
38. M.N. Nadagouda, N. Iyanna, J. Lalley, C. Han, D.D. Dionysiou, R.S. Varma, Synthesis of silver and gold nanoparticles using antioxidants from blackberry, blueberry, pomegranate, and turmeric extracts. Sustain. Chem. Eng. **2**, 1717 (2014)
39. L. Yang, D.H. Osborne, R.F. Haglund Jr., R.H. Magruder, C.W. White, R.A. Zuhr, H. Hosono, Probing interface properties of nanocomposites by third-order nonlinear optics. Appl. Phys. A. **62**, 403 (1996)
40. I.O. Sosa, C. Noguez, R.G. Barrera, optical properties of metal nanoparticles with arbitrary shapes. J. Phys. Chem. B **107**, 6269 (2003)
41. U. Kreibig, M. Vollmer, *Optical properties of metal clusters* (Springer, Berlin, 1995)
42. A. Mishra, S. Ram, Surface-enhanced optical absorption and photoluminescence in nonbonding electrons in small poly(vinylpyrrolidone) molecules. J. Chem. Phys. **126**, 084902 (2007)
43. A. Rout, G.S. Boltaev, R.A. Ganeev, Y. Fu, S.K. Maurya, V.V. Kim, K.S. Rao, C. Guo, Nonlinear optical studies of gold nanoparticle films. Nanomaterials **9**, 291 (2019)
44. K. Zhang, R.A. Ganeev, K.S. Rao, S.K. Maurya, G.S. Boltaev, P.S. Krishnendu, Z. Yu, W. Yu, Y. Fu, C. Guo, Interaction of pulses of different duration with chemically prepared silver nanoparticles:analysis of optical nonlinearities. J Nanomater **2019**, 6056528 (2019)
45. C.M. Aikens, S. Li, G.C. Schatz, From discrete electronic states to plasmons: TDDFT Optical Absorption Properties of Ag_n (n=10, 20, 35, 56, 84, 120) Tetrahedral Clusters. J. Phys. Chem. C **112**, 11272 (2008)
46. S.K. Maurya, A. Rout, R.A. Ganeev, C. Guo, Effect of Size on the Saturable Absorption and Reverse SaturableAbsorption in Silver Nanoparticle and Ultrafast Dynamics at 400nm. J. Nanomater **2019**, 9686913 (2019)
47. H.H. Mai, V.E. Kaydashev, V.K. Tikhomirov, E. Janssens, M.V. Shestakov, M. Meledina, S. Turner, G.V. Tendeloo, V.V. Moshchalkov, P. Lieven, Nonlinear optical properties of Ag nanoclusters and nanoparticles dispersed in a glass host. J. Phys. Chem. C. **118**, 15995 (2014)